Accepted Manuscript

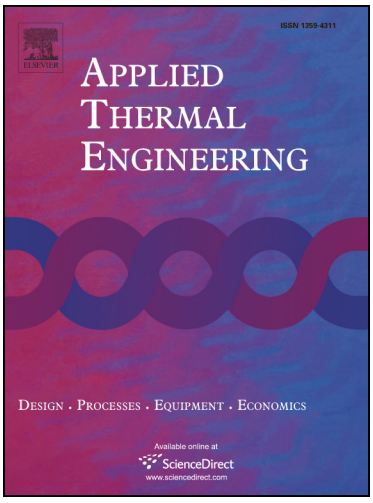

Research Paper

Identifying heterogeneities in cooling and quality evolution for a pallet of packed fresh fruit by using virtual cold chains

Wentao Wu, Thijs Defraeye

PII: S1359-4311(16)33849-2
DOI: https://doi.org/10.1016/j.applthermaleng.2017.11.049
Reference: ATE 11419

To appear in: *Applied Thermal Engineering*

Received Date: 2 December 2016
Revised Date: 11 October 2017
Accepted Date: 9 November 2017

Please cite this article as: W. Wu, T. Defraeye, Identifying heterogeneities in cooling and quality evolution for a pallet of packed fresh fruit by using virtual cold chains, *Applied Thermal Engineering* (2017), doi: https://doi.org/10.1016/j.applthermaleng.2017.11.049

Identifying heterogeneities in cooling and quality evolution for a pallet of packed fresh fruit by using virtual cold chains

Wentao Wu[1,2], Thijs Defraeye [1, 2*]

[1] *Chair of Building Physics, ETH Zurich, Stefano-Franscini-Platz 5, 8093 Zürich, Switzerland*

[2] *Multiscale Studies in Building Physics, Empa, Überlandstrasse 129, 8600 Dübendorf, Switzerland*

Abstract

Temperature control of fresh produce by forced convective cooling through ventilated packaging is essential to preserve quality in postharvest supply chains. The challenge is to achieve uniform cooling of fruit in the entire cargo. Most numerical research using computational fluid dynamics (CFD) focused on ventilated packaging with relatively small ensembles of fruit. This study aims to gain more insight into the thermal heterogeneity and the associated differences in quality evolution for large ensembles of packed fruit, by investigating the thermal behavior of an entire pallet of fruit throughout the entire cold chain. To this end, the virtual cold chain method is applied, which virtually tracks the temperature-time history of individual fruit using CFD and accordingly predicts fruit quality evolution using kinetic rate law models. The pallet includes 80 cartons, in which 5120 fruit are explicitly modelled as discrete spheres. Three cold chain scenarios are evaluated. For all the three unit operations in a cold chain (precooling, transport and

* Corresponding author. Tel. +41 (0)58 765 47 90

Email Address: thijs.defraeye@empa.ch (Thijs Defraeye)

storage), significant differences in the fruit cooling time are found along the airflow direction, where the blockage of local vent holes is found to increase the thermal heterogeneity. Cooling heterogeneity is the smallest for precooling and the largest for storage. Fruit in upstream cartons also show a higher heterogeneity than those in downstream cartons. The difference in quality evolution between individual fruit is found to be very limited if proper precooling is applied in the cold chain. In the cold chain without precooling, about 23% more quality loss is found than in that with precooling. Ambient loading is promising to remove field heat during refrigerated transport.

Keywords: virtual cold chain; cooling heterogeneity; quality evolution; pallet; citrus fruit

Highlight

- Heterogeneous airflow distribution in the pallet is visualised.
- Cooling heterogeneity along the airflow direction in a pallet is identified.
- Larger cooling heterogeneity among individual fruit occurs in upstream cartons.
- Difference in quality loss is small for fruit in cold chains with precooling.
- Cold chains without precooling have about 23% more quality loss.

1. Introduction

The loss of perishable foods due to lack of refrigeration ranges from 9% in developed countries to 23% in developing countries (IIR, 2009). Over 360 million tonnes (Billiard, 1999) of perishable foods are lost worldwide each year. In the case of fresh fruit, the postharvest loss, from the point of harvest until they reach the consumer, can become as high as 38% of the total produced volume (Gustavsson et al., 2011). These huge losses can be minimized by proper temperature control, namely via refrigeration throughout the cold

chain since temperature is the single most important factor that affects fruit quality, deterioration rates and shelf life (Thompson et al., 2008). Forced air convection cooling is widely used to precool fresh fruit in ventilated packaging and to maintain fruit at optimum temperature during subsequent transport and storage. A problem with forced air convection cooling is that significant cooling heterogeneity between individual fruit in the cargo is often found. O'Sullivan et al. (2016) identified such cooling heterogeneity in palletised kiwifruit packages undergoing forced-air precooling. Han et al (2015) revealed the complex and uneven distribution of airflow and temperature fields inside a vented package with two layers of stacked produce. Defraeye et al (2015) and Delele et al. (2013) reported a large cooling heterogeneity between individual boxes at different heights on a pallet and also between individual fruit within a single box. More previous work has also identified the cooling heterogeneity between individual fruit (Defraeye et al., 2013, Ferrua and Singh, 2009a, b, c & 2011, Delele et al., 2008, Laguerre et al., 2006, Moureh and Flick, 2004, Alvarez and Flick, 1999a&b). Due to the fact that the temperature-time history of the fruit can be directly related to produce quality loss (Robertson, 1993), non-uniform cooling will induce heterogeneities in quality evolution of individual fruit. To provide retailers and customers with a uniform product quality within the batch that they purchase, reducing cooling heterogeneity is imperative. Furthermore, temperatures are only measured at a few locations in the cargo, uniform cooling is therefore critical for these temperatures to be representative for the entire cargo.

An important factor affecting cooling heterogeneity is the ventilated package design (Berry et al., 2017) and their stacking pattern on the pallet (Fig. 1). Ventilated packaging for fresh fruit, such as cartons for citrus or pome fruit, is commonly designed with ventilation

openings, which allow cold air to access the fruit. The limited number of vent holes and the blockage of vent holes due to stacking of the cartons on a pallet lead to a complex and heterogeneous airflow distribution within the cartons. Fruit near vent holes on the inflow side are exposed to high air speeds and thereby are cooled the fastest. Too fast cooling is however not desirable as this can lead to chilling injury. On the other hand, fruit sheltered by the carton and in the cartons stacked more downstream behind other cartons are cooled normally much slower.

A lot of valuable research has been done to analyse the heat flow within packaging filled with products using computational fluid dynamics (CFD). Zhao et al. (2016) and Ambaw et al. (2013) reviewed the application of CFD to analyse forced convection cooling of horticultural products and confirmed the value of CFD as an efficient tool for modelling of transport phenomena inside complex packaging structures. Most of the current modelling work focused on studying the forced convective cooling of a single package (Delele et al., 2013 & 2008, Dehghannya et al., 2011, Laguerre et al., 2008, Opara and Zou, 2007) or a small ensemble of packages (a horizontal layer or a vertical column of a pallet) (Defraeye et al., 2013, Ferrua and Singh, 2011). Only a single unit operation of the cold chain (Pathare et al, 2012) was targeted, such as precooling, transport in refrigerated containers or cold storage. Subsequent association of the cooling heterogeneity to the heterogeneity in quality evolution between the individual fruit is however barely investigated. To tackle these aspects, a virtual cold chain approach (VCC) (Wu et al., 2016) has been developed recently, which enables to calculate the temperature-time history of each individual fruit in the package, and to link temperature data to quality evolution throughout all unit operations of a cold chain. The fruit temperature-time history is calculated using CFD and a kinetic

rate-law model is used to determine the fruit quality evolution. The VCC method has been applied so far to a single carton with 64 citrus fruit, but provides the potential to analyze much larger batches of fruit. This is of large interest since evaluating the temperature and quality evolution within an entire pallet of fruit comes much closer to commercial practice than a single carton of fruit. Computational modelling of an entire pallet of packed fresh fruit using the VCC method will provide more realistic insights on cooling uniformity and fruit quality evolution of the cargo throughout the entire cold chain.

The objective of this study is to understand the heterogeneity in airflow, cooling behavior and quality evolution of individual fruit, packed in ventilated cartons on an entire pallet, for different cold chain scenarios. The VCC method will be applied to this pallet, containing 5120 fruit packed in 80 cartons. To our best knowledge, this is the first computational study that tracks the thermal behavior and quality evolution of an entire pallet of fruit, where each fruit is discretely modelled and monitored during precooling, refrigerated transport and cold storage unit operations.

2. Materials and methods

2.1. VCC method

In the first step of the VCC method (Wu et al., 2016), a detailed geometrical model for a pallet is created, which includes cartons and fruit (see section 2.2). Computational models (see section 2.3) are then built for the different unit operations (precooling, transport, storage). In the next step, calculations of air and heat flow through the pallet and heat transfer within the fruit are performed for each of the unit operations in the cold chain (see section 2.4). Here, the temperature distribution of each single fruit is transferred from one

virtual unit operation (e.g., precooling) to the next (e.g., transport). In the final step, the kinetic rate-law model (see section 2.5) is applied to calculate the produce quality evolution using the temperature-time history of individual fruit, extracted from all virtual unit operations. The same procedure is repeated for different cold chain scenarios (see section 2.6).

2.2. Packaging and palletisation

A telescopic corrugated fibreboard carton is used (0.4 m ×0.3 m ×0.27 m, see Fig. 2a). The carton has two circular vent holes on each lateral side, at half height. During precooling and storage, these side vent holes enable horizontal airflow (Fig. 2a). The carton has four circular vent holes and a rectangular slot on top and bottom surfaces, respectively, which enable vertical airflow during refrigerated transport (Fig. 2a). The carton is filled with 64 citrus fruit according to a predetermined staggered pattern, which is commonly adopted in citrus industry during packaging. Fruit are discretely modelled as spheres with a diameter of 75 mm. To avoid the generation of highly skewed meshing cells near the contact point of two fruit, a gap of about 3 mm is left between the fruits. Similar distances were adopted by Ferrua and Singh (2008 & 2009a).

Eighty cartons are stacked to assemble a high-cube pallet (1.2 m ×1.0 m ×2.16 m) (Fig. 2b). This leads to 3 columns (Col1, Col2 and Col3) along the flow direction for precooling and storage, and 8 layers (L1-L8) along the flow direction for refrigerated transport. The pallet holds 5120 citrus fruit in total. Each layer contains 10 cartons (C01-C10). For each layer, Col1 and Col2, respectively, have 3 cartons, whereas Col3 has 4 cartons (Fig. 3). The 3-3-4 configuration of the 10 cartons results in the blockage of lateral vent holes at the interface

of Col2 and Col3 (Fig. 3). The total vent area is reduced to 33% of the available vent area at this interface. The 8 layers are stacked regularly on top of one another (Fig. 2b).

2.3. Computational domain and mesh

Three separate computational models (Fig. 4) are constructed for precooling, transport and storage, respectively. In the models for precooling and cold storage, the pallet is ventilated horizontally (Fig. 4a), while in the model for refrigerated transport, the pallet is ventilated vertically (Fig. 4b). The upstream and downstream sections are extended sufficiently long to reduce the impact of inlet and outlet boundary conditions on the flow near the proximity of the pallet.

All CFD models are meshed using tetrahedral cells. The mesh for precooling and storage consists of 26.0×10^6 cells and that for transport has 25.4×10^6 cells. Tetrahedral cells are placed on both sides of the fruit surface. The wall y^+ is below 185, 6 and 3 for precooling, transport and storage, respectively. The spatial discretisation error is estimated by means of Richardson extrapolation (Roache, 1994), which is about 2.5% for the mass flow rate through the carton and 5% for the convective heat transfer coefficient on the citrus fruit surfaces.

2.4. Model development

Buoyancy is not modelled in this study, as forced convective airflow is considered. Therefore, the airflow within the cartons is a steady, turbulent and incompressible fluid flow of dry air with constant density. Under these flow conditions, the continuity equation and Reynolds-averaged Navier-Stokes (RANS) equations for steady and incompressible

flow are solved.

$$\frac{\partial U_i}{\partial x_i} = 0 \tag{1}$$

$$\rho U_j \frac{\partial U_i}{\partial x_j} = \frac{\partial P}{\partial x_i} + \mu \frac{\partial^2 U_i}{\partial x_j \partial x_j} + \frac{\partial(-\rho\overline{u_i' u_j'})}{\partial x_j} + S_M \tag{2}$$

where U_i is mean air velocity component in the x_i direction [m s^{-1}], x_i is Cartesian coordinate, ρ is density of air [kg m^{-3}], P is the air pressure [Pa], μ is the dynamic viscosity of air [kg m^{-1} s^{-1}] and S_M is source term for momentum. The Reynolds stress term is approximated by:

$$-\rho\overline{u_i' u_j'} = \mu_t \left(\frac{\partial U_i}{\partial x_j} + \frac{\partial U_j}{\partial x_i} \right) - \frac{2}{3} \rho k \delta_{ij} \tag{3}$$

where μ_t is the turbulent dynamic viscosity of air [kg m^{-1} s^{-1}] and k is the turbulent kinetic energy. The shear stress transport (SST) k-ω turbulence model (Menter, 1994) is used to close the RANS equations.

The temperature in the airflow and in the fruits is changing over time. Therefore, the transient energy equation for incompressible flow is calculated to obtain the air temperature field in between the individual fruit. This calculation is performed after the steady airflow calculation, as detailed below. Following transport equation is solved:

$$\frac{\partial T}{\partial t} + U_j \frac{\partial T}{\partial x_j} = \alpha \frac{\partial^2 T}{\partial x_j \partial x_j} + \frac{\partial(-\overline{T' u_j'})}{\partial x_j} + S_e \tag{4}$$

where T is the air temperature [K], t is the time [s], S_e is the source term, α is the thermal diffusivity [m^2 s^{-1}] and is calculated as follows:

$$\alpha = \frac{\lambda}{\rho C} \tag{5}$$

where λ is the thermal conductivity of air [W m^{-1} K^{-1}] and C is the specific heat capacity of air [J kg^{-1} K^{-1}].

The fluctuating term is approximated by:

$$-\overline{T'u_j'} = \alpha_t \frac{\partial T}{\partial x_j} \tag{6}$$

where α_t is turbulent thermal diffusivity [m^2 s^{-1}].

At the same time when this transient energy equation for incompressible flow is solved, the transient heat conduction equation in the fruits is calculated to obtain the temperature distribution inside the fruit.

$$\rho_s C_s \frac{\partial T_s}{\partial t} = \lambda_s \frac{\partial^2 T_s}{\partial x_j \partial x_j} + S_s \tag{7}$$

where ρ_s is the density of fruit [kg m^{-1} s^{-1}], C_s is the specific heat capacity of fruit [J kg^{-1} K^{-1}], λ_s is the thermal conductivity of fruit [W m^{-1} K^{-1}], T_s is the temperature field in fruit [K] and S_s is a source term.

The two energy equations are coupled by specifying continuity of heat flux and temperature at the fruit surfaces by the two following equations:

$$T_s(\boldsymbol{x}, t) = T(\boldsymbol{x}, t) \tag{8}$$

where $\boldsymbol{x}$ is the Cartesian coordinate of the fruit surface.

$$\boldsymbol{n} \cdot \lambda_s \nabla T_s(\boldsymbol{x}, t) = \boldsymbol{n} \cdot \lambda \nabla T(\boldsymbol{x}, t) \tag{9}$$

where $\boldsymbol{n}$ is the normal vector of the fruit surface at the position $\boldsymbol{x}$.

The steady Navier Stokes equations are solved first and in a next step the transient energy equations for both air and fruit are solved simultaneously to obtain the temperature distribution profiles in the air and the fruit. The two step approach is commonly used for forced-air cooling applications (Zhao et al., 2016; Han et al., 2015; Defraeye et al., 2013; Ferrua and Singh, 2009a).

The computational models for flow and temperature calculations were validated by many authors (Defraeye et al., 2013; Ambaw et al., 2013; Delele et al., 2009). Defraeye et al. (2013) carried out cooling experiments and CFD simulations on similar cartons, in which the number of fruit number, stacking patterns and diameter were similar to this study. The CFD results showed very good agreements with experiments. For the same turbulence models and geometrical models are used in the present study as well, but just on a larger scale (a pallet), the accuracy of the modelling is also assumed to be good.

2.5. Boundary conditions

At the outlet, a volumetric flow rate is imposed and its value depends on the specific cold chain unit operation. The flow rates (see Table 1) in the present study are 0.2, 0.02 and 0.002 L s^{-1} kg^{-1} of fruit for precooling, transport and storage, respectively. At the inlet, the atmospheric pressure is imposed with a low turbulence intensity of 0.1%. The inlet air temperature, or the so-called set-point temperature for the cold chain unit operation, varies with the different cold chain scenarios that are evaluated, and is given in Table 1. The lateral surfaces of the extended upstream and downstream sections and the vent holes on

the lateral cardboard surfaces of the pallet are treated as symmetry boundary conditions. The choice of the symmetry boundary condition is based on the assumption that each pallet has other pallets adjacent to it in all unit operations. The cardboard surfaces and the fruit surfaces are modelled as no-slip walls with zero roughness. Scalable wall functions (Menter and Esch, 2001) are used to model the flow and heat transfer in the boundary layer at the no-slip surfaces. This method switches automatically from a wall function to a low-Reynolds number formulation, based on the grid density. The accuracy of the SST k-ω turbulence model with wall function boundary-layer modelling was shown to be satisfactory by several previous studies (Defraeye et al., 2013; Ambaw et al., 2013; Delele et al., 2009).

2.6. Numerical methods

The simulations are performed with the open source CFD code OpenFOAM 2.4.0. The temperature difference between adjacent citrus fruit in the packaging is rather small during cooling. Therefore, radiation exchange between fruit inside the stack is considered limited compared to convective heat transfer (Defraeye et al., 2013) and hence, radiation is not modelled. Heat of respiration is about 50 W ton^{-1} for citrus fruit (ASHRAE, 1994) and the mass loss from citrus fruit in the cold chain is rather limited. Therefore, heat of respiration and latent heat of evaporation due to mass loss are unlikely to have a significant impact on the cooling rate of citrus fruit (Defraeye et al., 2013) and are not included in the model. The following thermal properties of citrus fruit are used in the simulations: density of 960 kg m^{-3}, thermal conductivity of 0.386 W $m^{-1}K^{-1}$ and specific heat capacity of 3850 J $kg^{-1}K^{-1}$.

The second-order upwind scheme is used to discretize the advection terms of the governing

equations. The first time derivative item is discretized by the first-order, bounded, implicit scheme Euler. The SIMPLE algorithm and merged PISO-SIMPLE (PIMPLE) algorithm are used for steady state and transient simulations, respectively.

The steady flow field calculation is firstly performed for each unit operation. On the basis of that, the transient heat transfer is resolved to obtain the temperature evolution. The initial temperature of the fruit and cardboard is taken equal to 21 ºC in this study. The transient simulations use a time step of 60 s, which is determined from the temporal sensitivity analysis.

2.7. Kinetic rate-law quality model

The kinetic rate-law quality model for the fruit is described in detail by Wu et al. (2016). Hence, only a brief summary is given here. A generic model for the change in overall fruit quality, indicated by parameter A, is developed based on a kinetic rate law (Robertson, 1993):

$$-\frac{dA}{dt} = kA^n \tag{10}$$

where t is the time [s], k is the rate constant [s^{-1}], n is the order of the reaction which determines whether the change of A over time is dependent on itself. A zero-order reaction is assumed in this study for the change of the overall quality A. This implies that the change of A over time is a linear curve, where the magnitude of the slope equals k. If Eq.(10) is integrated, a linear decrease of the quality parameter is found at a constant temperature (k is temperature dependent):

$$A = A_0 - kt \tag{11}$$

where A_0 is the quality at the start of a cold chain (t = 0 d). The temperature dependency of the degradation of fruit quality is accounted for by the rate constant k, which is often described by an Arrhenius relationship (Robertson, 1993):

$$k(T) = k_0 e^{\frac{-E_a}{RT}} \quad (12)$$

where k_0 is a constant [d^{-1}], E_a is the activation energy [J mol^{-1}], R is the ideal gas constant (8.314 J mol^{-1} K^{-1}), T is the absolute temperature [K]. The constant k_0 and E_a can be inferred from quality decay data.

According to Cantwell (2001), citrus fruit can be stored for approximately 56 d at 4 ºC. This means that the initial overall quality A_0 (100%) is assumed to be totally lost (the remaining quality A_{end} = 0%) after citrus fruit are stored for 56 d at 4 ºC. According to Robertson (1993), an increase in temperature of 10 °C halves the shelf life, which means citrus fruit can be stored for approximately 28 d at 14 ºC. Based on these quantities, the rate constants at 4 ºC and 14 ºC can be derived via Eq.(11). Using these two determined rate constants and Eq. (12), E_a and k_0 can be easily calculated, which equal 4.59 x 10^4 J mol^{-1} and 7.89 x 10^6 d^{-1}, respectively. After this calibration of the quality model with experimental data, the temperature dependency of the fruit quality can be predicted throughout the cold chain. Through such calibration, this model which is based on modeled temperatures, will yield similar quality predictions as the case where fruit would be subjected experimentally to the same temperature conditions.

As fruit temperature varies along the cold chain, the rate constant will also vary accordingly. The fruit core temperature is monitored to calculate the fruit quality change. The most important reason to choose the fruit core temperature, and not the volume-

averaged fruit temperature, is that the core temperature is now used in the citrus industry as the measured parameter, by inserting a point probe. In addition, the center of the fruit is typically the last location to reach the target temperature. Therefore, the use of the core temperature to assess fruit quality is the most conservative scenario. Eq.(12) and Eq.(11) is then used to calculate the rate constant for each time interval and the cumulative remaining quality at each time step, respectively.

2.8. Different cold chains

Wu et al. (2016) evaluated five cold chain scenarios for a single carton to mimic the different postharvest supply chain strategies used in the citrus fruit industry in South Africa. Three of these cold chain scenarios (see Table 1) are assessed in this study for a pallet. The main focus is to unveil the differences between cases with and without precooling. The baseline cold chain includes precooling (1 d at 3 °C), transport at a temperature regime for cold disinfestation (24 d at -1 °C) and cold storage (14 d at 4 °C). This case simulated direct removal of the majority of the field heat by precooling and then further heat removal during transport. The second cold chain 'ambient cooling' does not include precooling. Instead, fruit are held in normal cold storage for 5 d at 3 °C before shipment, which induces a slow cooling process. Afterwards, the fruit are placed in refrigerated transport (24 d at -1 °C) and cold storage (14 d at 4 °C) after shipment. In the last cold chain, 'ambient loading' (Defraeye et al., 2015), the fruit are directly loaded to the refrigerated container after being packed. After 24 d of transport at -1 °C, the fruit are held in cold storage for 14 d at 4 °C. Such ambient loading is used in South Africa to shorten the cold chain and to enable more cooling capacity in regions where there is insufficient precooling capacity.

2.9. *Evaluation of cooling rate*

The cooling rate of each fruit is assessed by the temperature-time history, monitored in the center of the citrus fruit. From these temperature profiles (T [K]) the fractional unaccomplished temperature change (Y) can be determined (Defraeye et al., 2015).

$$Y = \frac{T - T_a}{T_i - T_a} \tag{13}$$

where subscripts i and a represent the initial temperature of the fruit and the set point temperature in the associated cold chain unit operations, respectively. From the definition of Y, the seven eighths cooling/heating time ($t_{7/8}$) can be determined. The $t_{7/8}$ is the time required to reduce the temperature difference between the fruit and the set point air temperature by seven eighths (Y=0.125). More detailed explanation on this parameter can be found in the work of Defraeye et al. (2015).

3. Results

3.1. *Airflow inside the pallet*

Fig. 5 shows the airflow patterns inside the cartons in the pallet for precooling, transport and storage. Heterogeneous airflow distributions are predicted for all the three unit operations. The portion of the transversal flow from one layer to another during horizontal flow and from one column to another during vertical flow was found to be small compared to the inlet flow rate. The detailed spatial variations in air speed inside the pallet are further explored by sampling local air speeds at different distances from the inflow vent holes for the relevant unit operation (Y positive for precooling and storage, and Z positive for transport). For precooling and storage, air speeds are sampled along 6 lines (Fig. 6) at Z=0.135 m (the centre height of the vent holes, see Fig. 2a). For transport, air speeds are

sampled along 2 lines (Y=0.077 and 0.15 m in Fig. 6) at 4 heights Z=0.001, 0.077, 0.135 and 0.269 m. The reason for the choice of the sampling locations is that the heterogeneity in airflow along flow direction can be demonstrated. The air speed profiles at these locations are shown in Fig. 7.

For precooling (Fig. 7a-c), the airflow passes through the 6 vent holes at the inflow side of the pallet and enters into cartons C01-C03 as 6 jets (Fig. 7a). The speed profiles of the 6 jets are almost identical. The fruit in the vicinity of the 6 jets are exposed to high air speeds (5 m/s). The air speeds are much lower around the fruit further away from these vent holes. Along the flow direction (at Y=0.15 m), the magnitude of the 6 jets decreases in a similar manner. Deeper inside the pallet (at Y=0.377 m), two more peaks (near X=0.4 and 0.8 m) occur in the air speed profile (Fig. 7b). This is due to the fact that the downstream vent holes of carton C05 are totally blocked by cartons C08 and C09 (Fig. 3), causing the airflow to leave C05 through the two lateral side vent holes (X=0.4 and 0.8 m). Due to the blockage of vent holes, airflow enters C07 and C10 through only a single vent hole (Fig. 3), respectively. This is the reason for presence of two extreme high peaks (20.7 m/s) in the airflow profile along Y=0.663 m (Fig. 7c). The airflow is distributed into C08 and C09 through lateral side vent holes. The arrangement of 10 cartons on one horizontal layer (Fig. 3) blocks several vent holes and thereby leads to a more heterogeneous airflow distribution.

For transport (Fig. 7d-f), fruit in the cartons close to inflow vent holes are exposed to high airflow speed (Fig. 7d). When the airflow is further distributed into the cartons, the influence of the number and position of vent holes on the air speed profiles is still there but is more limited (Fig. 7e). The air speed profile at Z=0.001 m shows the speed distribution

just after air enters cartons C01-C03, whereas the profile at Z=0.269 m shows the speed distribution just before air leaves cartons C01-C03. These profiles collapse to each other (Fig. 7f). This demonstrates a periodical airflow patterns between different layers, which is due to the regular carton stacking in the pallet in this study. A more complicated carton (Fig. 1) stacking, as in practice, would cause partial blockage of vent holes on the interface of different layers and might introduce more heterogeneity in airflow distribution.

For storage (Fig. 7g-i), air speeds in the pallet are very low (below 0.2 m/s). Compared with precooling, the magnitude of inlet jets is lower (Fig. 7g). There is a clear dependency of the air speed profile along the lines with the airflow rate. Along the flow direction, airflow becomes more uniform after the first row of fruit. In C05, the highest airflow velocity occurs near the lateral side vent holes (near X=0.4 and 0.8 m) (Fig. 7h). Dead zones are formed inside C07-C10 due to the blockage of the vent holes (Fig. 7i).

3.2. Thermal heterogeneity in the pallet

The spatial distribution of the seven-eighths cooling time ($t_{7/8}$) for each carton is used to evaluate the cooling heterogeneity in a pallet throughout all unit operations of the baseline cold chain. The $t_{7/8}$ for each carton is calculated based on the mean core temperature of all fruit in that carton and the average $t_{7/8}$ per carton is shown in Fig. 8. For the precooling unit operation, the difference in spatial distribution of $t_{7/8}$ occurs along the flow direction (Fig. 8a). The fruit in the upstream cartons (C01-C03) cool faster and the $t_{7/8}$ is about 0.25 d. The fruit in the cartons C08 and C09 cool slowest due to the blockage of vent holes at the interface of C08-09 and C5 (Fig. 3), and the $t_{7/8}$ for these fruit are about 0.53 d. This result is in line with the airflow analysis. There are no heterogeneities in the spatial distribution of

$t_{7/8}$ along height (z direction). For transport, the differences in $t_{7/8}$ also appear mainly along the flow direction (Fig. 8b). The $t_{7/8}$ depends on the distance from the fruit to the inflow vent holes. The $t_{7/8}$ for the fruit in cartons on the same layer are approximately identical. For storage, the distribution of $t_{7/8}$ in the pallet is similar to the results for precooling. The $t_{7/8}$ for C05 are about 5 d longer than those for C04 and C06 (Fig. 8c).

From precooling, transport to storage, $t_{7/8}$ becomes increasingly larger, which clearly demonstrates that the airflow rate influences the cooling rate. For all the three unit operations, the cooling heterogeneity in the pallet appears along the flow direction and blockage of vent holes increases the heterogeneity. In order to clearly illustrate the dependence of cooling heterogeneity in the pallet on flow direction, the spatial distribution of $t_{7/8}$ is mapped schematically horizontally (during precooling and storage) and vertically (during transport) to the pallet, respectively (Fig. 8d).

3.3. Thermal heterogeneity in individual cartons

The cooling heterogeneity between individual fruit in two different cartons (L1C03 and L8C09, Fig. 9d) inside the pallet is assessed by evaluating the core temperature-time history (Fig. 9a-c) of each individual fruit. The choice of L1C03 and L8C09 is based on the spatial distribution of $t_{7/8}$ inside the pallet (Fig. 8), which shows that fruit in L1C03 cools the fastest and fruit in L8C09 cools the slowest. The differences between minimum and maximum $t_{7/8}$ for individual fruit in L1C03 are 0.14 d, 0.70 d and 9.30 d for precooling, transport and storage, respectively, while differences for individual fruit in L8C09 are 0.11 d, 0.46 d and 7.10 d for precooling, transport and storage, respectively. The difference between the minimum $t_{7/8}$ for fruit in L8C09, so the fastest cooling fruit in the pallet for that

unit operation, and the maximum $t_{7/8}$ for fruit in L1C03, so the slowest cooling fruit for that unit operation, is 0.16 d, 1.76 d and 18.90 d in precooling, transport and storage, respectively. The difference in the core temperatures between the two cartons becomes larger from precooling to transport and even larger from transport to storage. The increasingly larger cooling heterogeneity is caused by the lower airflow rates in the subsequent unit operation.

Compared with the fruit in L8C09, the fruit in L1C03 cool 2-4 times faster depending on the unit operation under consideration. During precooling, the $t_{7/8}$ varies from 0.18 d to 0.22 d for individual fruit in L1C03, whereas for L8C09, the $t_{7/8}$ lies between 0.48 d and 0.59 d. During transport, the $t_{7/8}$ for individual fruit varies from 0.39 d to 1.04 d in L1C03 but from 2.80 d to 3.20 d in L8C09. During storage, the $t_{7/8}$ for individual fruit lies between 4.90 d and 14.20 d in L1C03 but between 33.00 d and 40.00 d in L8C09.

The cooling heterogeneity in the entire pallet appears along the flow direction (Fig. 8). However, the spread of core temperature profiles for upstream cartons L1C03 is larger than that for downstream cartons L8C09.

3.4. Heterogeneity in fruit quality evolution

The quality evolution of individual fruit in cartons L1C03 and L8C09 is presented separately for the three cold chains – baseline, ambient cooling and ambient loading (Fig. 10). During precooling in the baseline cold chain, the quality loss for fruit in L1C03 and L8C09 does not show a significant difference. A slightly larger quality loss is present for the fruit in L8C09 after the start of the transport unit operation. From the point of storage,

fruit in L8C09 have less quality loss compared to those in L1C03. Since the set point temperature is higher during storage (4 °C) than during transport (-1 °C), the fruit are slightly heated when transferred from transport to storage. The transport temperatures are lower for the required cold disinfestation protocol. The fruit in L8C09 are the slowest to change temperature again, and the slow temperature change leads to less quality loss, which is actually beneficial. The remaining quality ranges from 44% to 47% for individual fruit in L1C03 and is about 49% for all individual fruit in L8C09. The significant cooling heterogeneity among cartons in a pallet (Fig. 8) and among individual fruit in the cartons (Fig. 9) does not lead to a large heterogeneity in quality loss for the baseline cold chain. One reason for the small variation of quality loss is the use of precooling. Precooling can swiftly remove the field heat and reduce the fruit temperature. During the long period of transport and storage, fruit temperature varies below a small range (below 5 °C) and thus the difference of temperature-related quality loss is also insignificant for individual fruit in a cold chain with proper precooling.

In the ambient cooling cold chain, the quality loss for fruit in L1C03 ranges from 15% to 25% after storage before shipment, which indicates a large spread. The quality loss for all individual fruit in L8C09 are around 35% and heterogeneity in quality loss for individual fruit in L8C09 is not significant. The end quality of individual fruit ranges from 25% to 33% in L1C03 and from 17% to 19% in L8C09. Fruit in L8C09 have lower end quality but also lower heterogeneity in quality evolution compared to fruit in L1C03. The ambient cooling cold chain has the lowest remaining quality. On average, about 23% more quality loss is found than in the baseline cold chain. The ambient cooling cold chain also shows the largest spread in quality evolution for individual fruit in the pallet.

In the ambient loading chain, the profiles of quality evolution for individual fruit in L1C03 are very similar to those in the baseline cold chain. An obvious deviation occurs in the beginning for quality evolution of individual fruit in L8C09 in the ambient loading cold chain, compared to the baseline cold chain. The reason is that the airflow rate (0.02 L $kg^{-1}s^{-1}$) during transport removes the field heat slower. The end quality of individual fruit ranges from 44% to 47% in L1C03 and from 45% to 48% in L8C09. The ambient loading cold chain has similar end quality, on average, compared to the baseline cold chain. Although the airflow rate during refrigerated transport is lower than that during precooling, it takes only about two and a half days longer to cool the fruit until the target temperature. The slightly larger quality loss during these few days are, however, compensated by the shorter duration of the cold chain, since faster shipping can be performed as fruit do not need to spend time in the precooler. Therefore, the ambient loading has comparable quality evolution in the cold chain, in comparison to the precooling treatment.

4. Conclusion

The virtual cold chain method was used to study the heterogeneity in cooling and quality evolution of packed fresh fruit in a pallet for three cold chain scenarios. The main conclusions were the following:

- The airflow distribution in the pallet was quite heterogeneous. Fruits close to vent holes were exposed to airflow with high speeds. The blockage of vent holes led to a more heterogeneous airflow distribution.
- For all the three unit operations (precooling, transport and storage), variations in the spatial distribution of seven eighths cooling/heating time appeared along the flow

direction and the fruit in the upstream cartons cooled faster. Blockage of vent holes increased the thermal heterogeneity.

- Cooling heterogeneity was the smallest for precooling and the largest for storage, due to the lower airflow rates in storage.
- Larger thermal heterogeneity occurred among individual fruit in upstream cartons, compared to downstream cartons.
- The variation in temperature-related quality loss was limited for individual fruit in a cold chain with proper precooling. The ambient cooling cold chain without precooling had about 23% more quality loss on average than that from the precooling-based cold chain. Ambient loading was found to be a promising alternative to direct precooling to remove field heat during refrigerated transport.

The combined modelling of temperature-time history with quality evolution for each individual fruit, using the virtual cold chain method, enables to unveil in a unique way significant differences in cooling behavior and fruit quality between cold chains. This study focused on one package type. Future studies will be directed to assess the impact of different packaging types on the cooling heterogeneity and quality loss, and also to look at other cold chain scenarios.

Acknowledgements

The authors would like to thank the Coop Research Program of the ETH Zurich World Food System Center and the ETH Foundation for supporting this project.

References

Alvarez, G., Flick, D., 1999a. Analysis of heterogeneous cooling of agricultural products inside bins part I: aerodynamic study. Journal of Food Engineering 39, 227-237.

Alvarez, G., Flick, D., 1999b. Analysis of heterogeneous cooling of agricultural products inside bins: part II: thermal study. Journal of Food Engineering, 39(3), 239-245.

Ambaw, A., Delele, M.A., Defraeye, T., Ho, Q.T., Opara, U.L., Nicolaï, B.M., Verboven, P., 2013. The use of CFD to characterize and design post‐harvest storage facilities: Past, present and future. Computers and Electronics in Agriculture 93, 184-194.

ASHRAE, 1994. ASHRAE Handbook - Refrigeration: systems and applications (SI edition). ASHRAE, Atlanta, USA.

Berry, T., Fadiji, T., Defraeye, T., Opara, U., 2017. The role of horticultural carton vent hole design on cooling efficiency and compression strength: A multi-parameter approach. Postharvest Biology and Technology 124, 62-74.

Billiard, F., 1999. New Developments in the Food Cold Chain Worldwide. Proc. 20th Int. Congr. Refrig., Sydney.

Cantwell, M., 2001. Properties and recommended conditions for long-term storage of fresh fruits and vegetables, UC Davis.

Dehghannya, J., Ngadi, M., Vigneault, C., 2011. Mathematical modeling of airflow and heat transfer during forced convection cooling of produce considering various package vent areas, Food Control 22 (8), 1393-1399.

Dehghannya, J., Ngadi, M., Vigneault, C., 2012. Transport phenomena modelling during produce cooling for optimal package design: Thermal sensitivity analysis. Biosystems Engineering 111 (3), 315-324.

Defraeye T., Lambrecht R., Ambaw A., Delele M.A., Opara U.L., Cronjé P., Verboven P., Nicolai B., 2013. Forced-convective cooling of citrus fruit: package design, Journal of Food

Engineering 118 (1), 8-18.

Defraeye T., Verboven P., Opara U.L., Nicolai B., Cronjé P., 2015. Feasibility of ambient loading of citrus fruit into refrigerated containers for cooling during marine transport, Biosystems Engineering 134, 20-30.

Delele, M.A., Tijskens, E., Atalay, T.A., Ho, Q.T., Ramon, H., Nicolaï, B.M., Verboven, P., 2008. Combined discrete element and CFD modeling of airflow through random stacking of horticultural products in vented boxes. Journal of Food Engineering 89, 33-41.

Delele, M.A., Schenk, A., Ramon, H., Nicolaï, B.M., Verboven, P., 2009. Evaluation of a chicory root cold store humidification system using computational fluid dynamics. Journal of Food Engineering 94, 110-121.

Delele, M.A., Ngcobo, M., Getahun, S., Chen, L., Mellmann, J., Opara, U., 2013. Studying airflow and heat transfer characteristics of a horticultural produce packaging system using a 3-D CFD model. Part I: model development and validation, Journal of Food Engineering 86 (12), 536-545.

Ferrua, M.J., Singh, R.P., 2008. A nonintrusive flow measurement technique to validate the simulated laminar fluid flow in a packed container with vented walls. International journal of refrigeration 31, 242-255.

Ferrua, M.J., Singh, R.P., 2009a. Modeling the forced-air cooling process of fresh strawberry packages, Part I: numerical model. International Journal of Refrigeration 32, 335-348.

Ferrua, M.J., Singh, R.P., 2009b. Modeling the forced-air cooling process of fresh strawberry packages, Part II: experimental validation of the flow model. International Journal of Refrigeration 32, 349-358.

Ferrua, M.J., Singh, R.P., 2009c. Modeling the forced-air cooling process of fresh

strawberry packages, Part III: experimental validation of the energy model. International Journal of Refrigeration 32, 359-368.

Ferrua, M.J., Singh, R.P., 2011. Improved airflow method and packaging system for forced-air cooling of strawberries. International Journal of Refrigeration 34, 1162-1173.

Gustavsson, J., Cederberg, C., Sonesson, U., van Otterdijk, R., Meybeck, A., 2011. Global food losses and food wastes – extent, causes and prevention (www.fao.org). Rome, Italy.

Han, J., Zhao, C., Yang, X., Qian, J., Fan, B., 2015. Computational modeling of airflow and heat transfer in a vented box during cooling: Optimal package design. Applied Thermal Engineering 91, 883-893.

IIR, 2009. 5th Informatory Note on Refrigeration and Food: The Role of Refrigeration in Worldwide Nutrition (www.iifiir.og).

Laguerre, O., Ben Amara, S., Flick, D., 2006. Heat transfer between wall and packed bed crossed by low velocity airflow. Applied Thermal Engineering 26 (16), 1951-1960.

Laguerre, O., Ben Amara, S., Alvarez, G., Flick, D., 2008. Transient heat transfer by free convection in a packed bed of spheres: Comparison between two modelling approaches and experimental results. Applied Thermal Engineering 28 (1), 14-24.

Menter, F.R., 1994. Two equation eddy viscosity turbulence models for engineering applications. AIAA Journal 32(8), 1598-1605.

Menter, F., Esch, T., "Elements of Industrial Heat Transfer Prediction", 16th Brazilian Congress of Mechanical Engineering (COBEM), Nov. 2001.

Moureh, J., Flick, D., 2004. Airflow pattern and temperature distribution in a typical refrigerated truck configuration loaded with pallets. International Journal of Refrigeration 27 (5), 464-474.

Opara, U., Zou, Q., 2007. Sensitivity analysis of a CFD modelling system for airflow and

heat transfer of fresh food packaging: inlet air flow velocity and inside package configurations, International Journal of Food Engineering 3 (5), 1556-3758.

O'Sullivan, J., Ferruaa, M., Love, R., Verboven, P., Nicolai, B., East, A., 2016. Modelling the forced-air cooling mechanisms and performance of polylined horticultural produce. Postharvest Biology and Technology 120, 23-35.

Pathare, P., Opara, U., Vigneault, C., Delele, M., Al-Said, A., 2012. Design of packaging vents for cooling fresh horticultural produce. Food and Bioprocess Technology 5, 2031-2045.

Roache, P., 1994. Perspective: a method for uniform reporting of grid refinement studies. Transactions of the ASME – Journal of Fluids Engineering 116 (3), 405-413.

Robertson, G.L., 1993. Food Packaging: Principles and Practices, Marcel Dekker, Inc., New York.

Thompson, J. F., Mitchell, F. G., Rumsey, R. T., Kasmire, R. F., & Crisosto, C. H., 2008. Commercial cooling of fruit, vegetables and flowers (p. 61). California: University of California.

Wu, W., Cronje, P., Nicolai, B., Verboven, P., Opara, U., Defraeye, T., 2016. Virtual cold chain to model the postharvest thermal history and quality evolution of fresh fruit – A case study for citrus fruit packed in a single carton. Submitted manuscript.

Zhao, C., Han, J., Yang, X., Qian, J., Fan, B., 2016. A review of computational fluid dynamics for forced-air cooling process. Applied Energy 168, 314-331.

Fig.1 Illustration of airflow for forced air precooling, storage (horizontal) and refrigerated transport (vertical) for an 8-layer, high-cube citrus pallet (10 standard cartons per layer).

Fig. 2 (a) Geometry and dimensions of the standard carton, packed with 64 oranges; (b) 8-layer (numbered from L1 to L8), 3-column (numbered from Col1 to Col3), high-cube citrus pallet (incl. 5120 fruit in total); 10 cartons (numbered from C01 to C10) per layer; 8 layers are regularly stacked.

Fig.3 Blockage of vent holes due to carton stacking, illustrated in layer L1.

Fig. 4 CFD models and boundary conditions for typical cold chain unit operations: precooling, refrigerated transport and cold storage.

Fig. 5 Airflow streamlines for precooling, refrigerated transport and cold storage.

Fig. 6 Air speed sampling lines (6 black thick lines, aligned with X axis), illustrated on layer L1 of the pallet. For precooling and storage, air speeds were sampled along Y=77, 150, 377, 450, 663 and 794 mm at Z=135 mm; for transport, air speeds were sampled along Y=77 and 150 mm at Z=1, 77, 135 and 269 mm. Y= 77 and 150 mm are behind the first and second row of fruit in the cartons C01-C03; Y=377 and 450 mm are behind the first and second row of fruit in the cartons C04-C06; Y=663 mm lies under the centre of the 8 top circular vent holes and Y=794 mm are under the 4 top rectangular vent holes in the cartons C07-C10.

Fig. 7 Air speeds sampled along different lines for precooling, refrigerated transport and cold storage.

Fig. 8 Spatial distribution of seven-eighth cooling/heating time ($t_{7/8}$) for each box during precooling, transport & storage. $t_{7/8}$ is based on average of core temperature of all fruit in a single carton.

Fig. 9 Core temperature-time history of each individual fruit in carton L1C03 and L8C09 during each unit operation (Precooling, transport and storage). $T_{t7/8}$- temperature at seven eighths cooling/heating time ($t_{7/8}$), that is, one eighths of set point temperature..

Fig. 10 Quality loss of individual fruit in cartons L1C03 and L8C09 (Fig. 9d) throughout the three cold chains – baseline, ambient cooling and ambient loading.

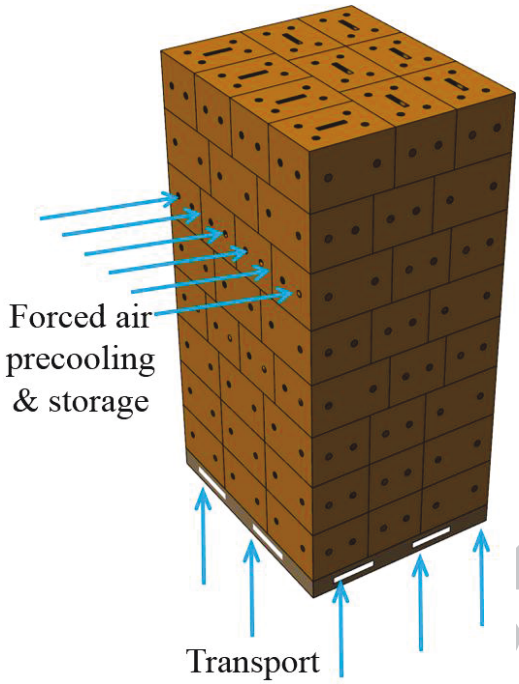

Fig.1 Illustration of airflow for forced air precooling, storage (horizontal) and refrigerated transport (vertical) for an 8-layer, high-cube citrus pallet (10 standard cartons per layer).

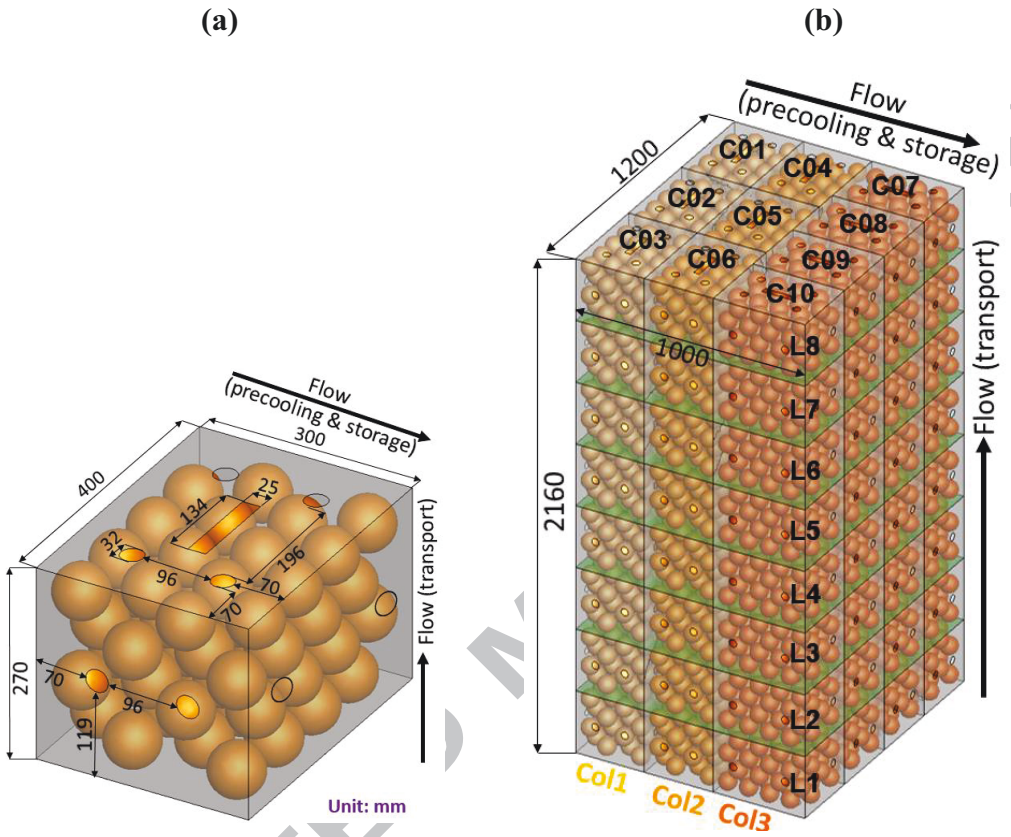

Fig. 2 (a) Geometry and dimensions of the standard carton, packed with 64 oranges; (b) 8-layer (numbered from L1 to L8), 3-column (numbered from Col1 to Col3), high-cube citrus pallet (incl. 5120 fruit in total); 10 cartons (numbered from C01 to C10) per layer; 8 layers are regularly stacked.

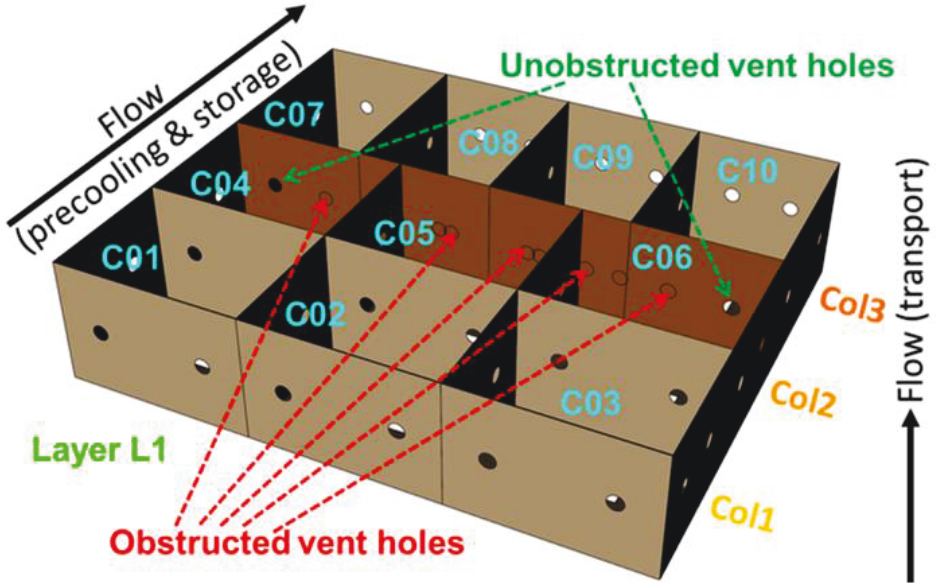

Fig.3 Blockage of vent holes due to carton stacking, illustrated in layer L1.

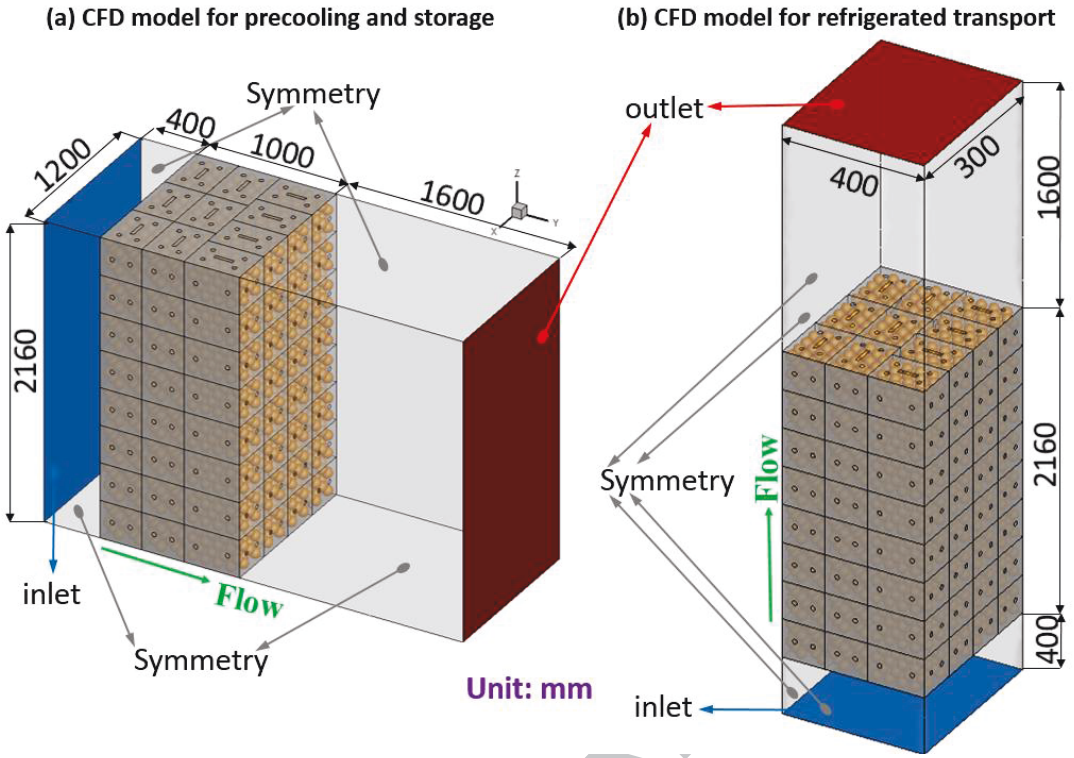

Fig. 4 CFD models and boundary conditions for typical cold chain unit operations: precooling, refrigerated transport and cold storage.

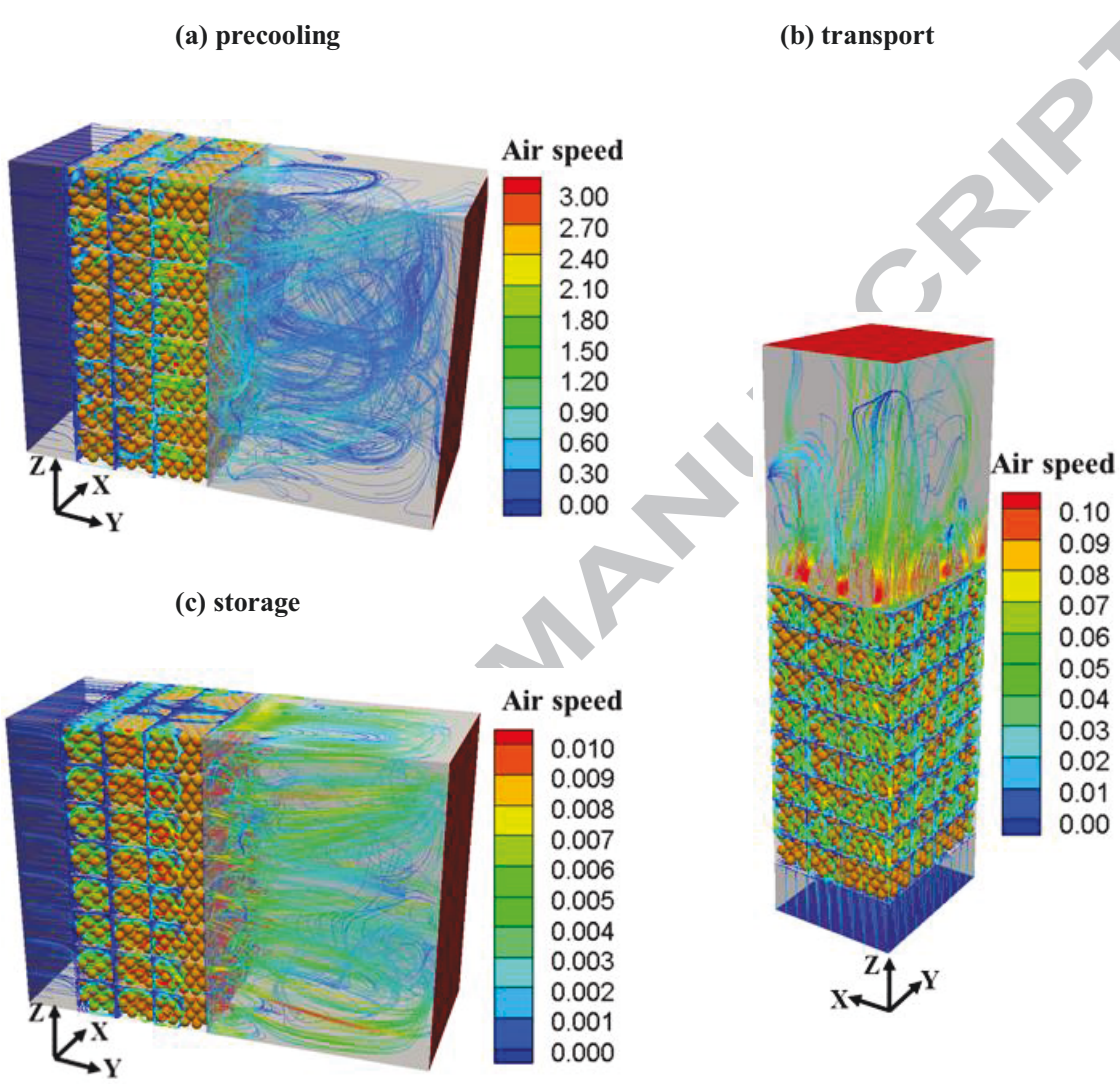

Fig. 5 Airflow streamlines for precooling, refrigerated transport and cold storage.

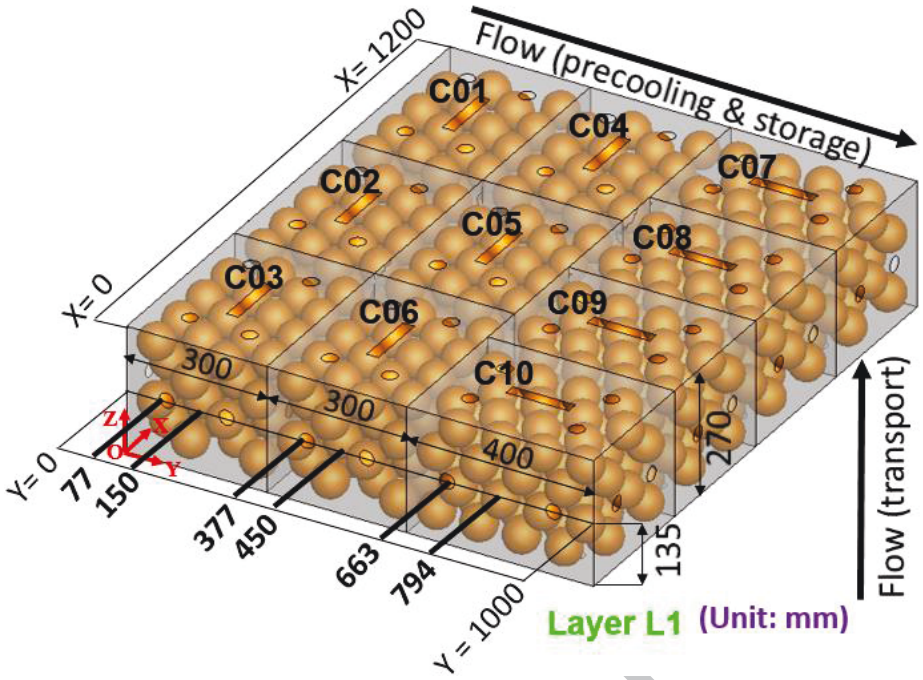

Fig. 6 Air speed sampling lines (6 black thick lines, aligned with X axis), illustrated on layer L1 of the pallet. For precooling and storage, air speeds were sampled along Y=77, 150, 377, 450, 663 and 794 mm at Z=135 mm; for transport, air speeds were sampled along Y=77 and 150 mm at Z=1, 77, 135 and 269 mm. Y= 77 and 150 mm are behind the first and second row of fruit in the cartons C01-C03; Y=377 and 450 mm are behind the first and second row of fruit in the cartons C04-C06; Y=663 mm lies under the centre of the 8 top circular vent holes and Y=794 mm are under the 4 top rectangular vent holes in the cartons C07-C10.

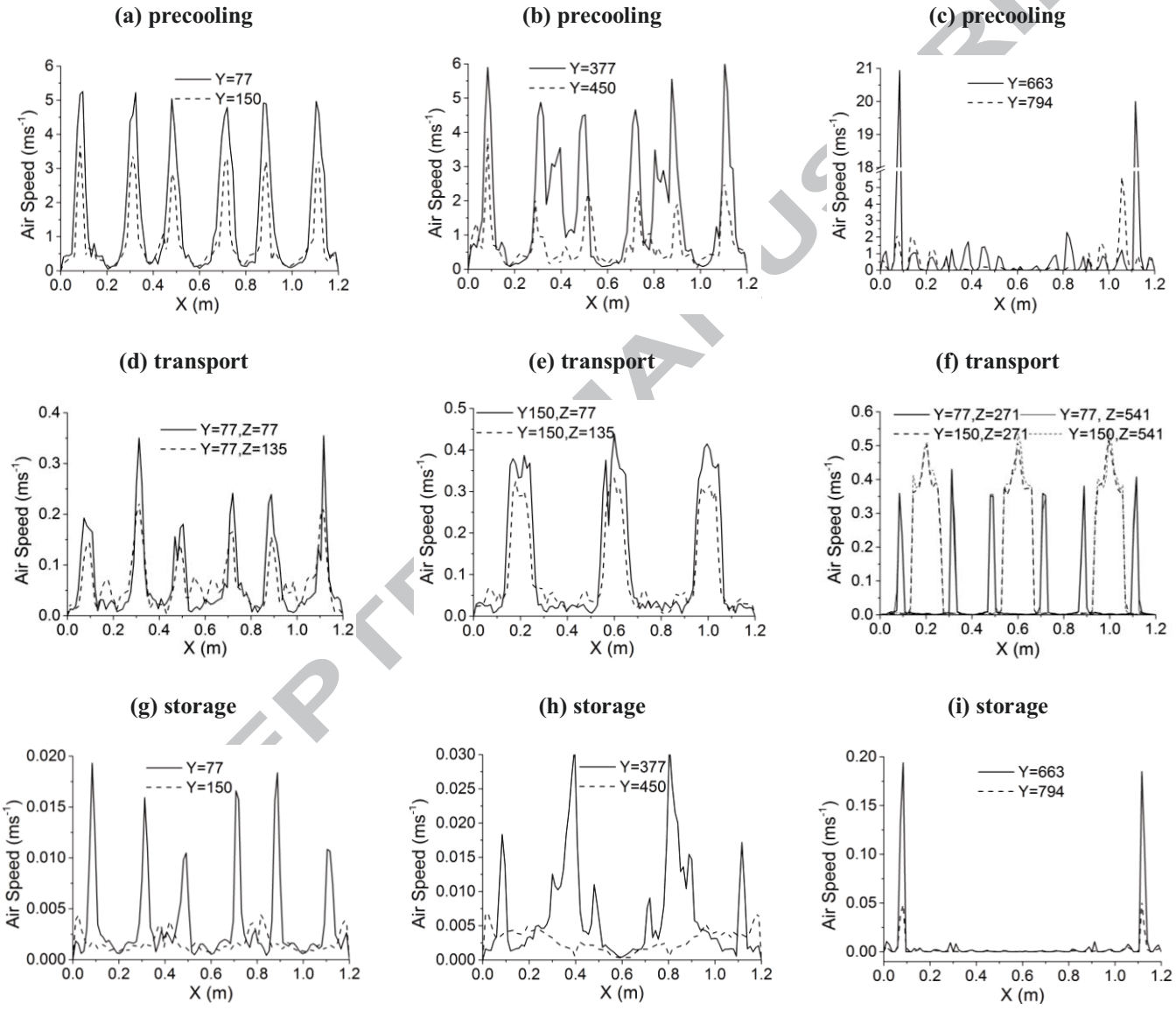

Fig. 7 Air speeds sampled along different lines for precooling, refrigerated transport and cold storage.

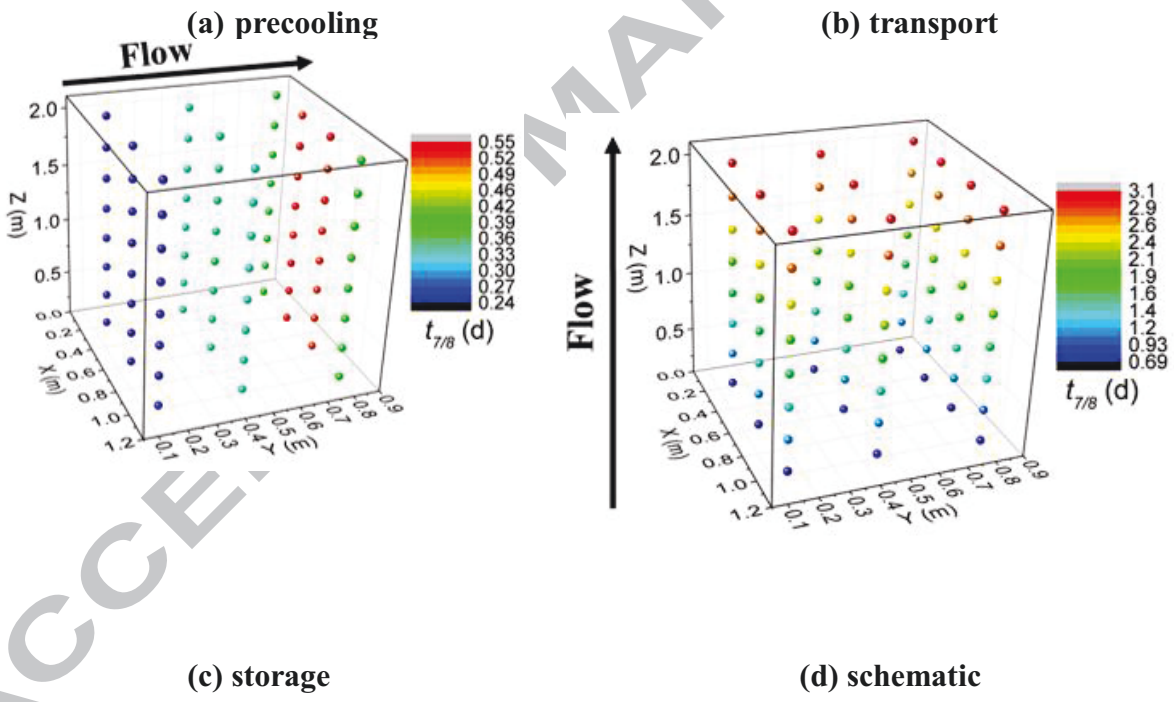

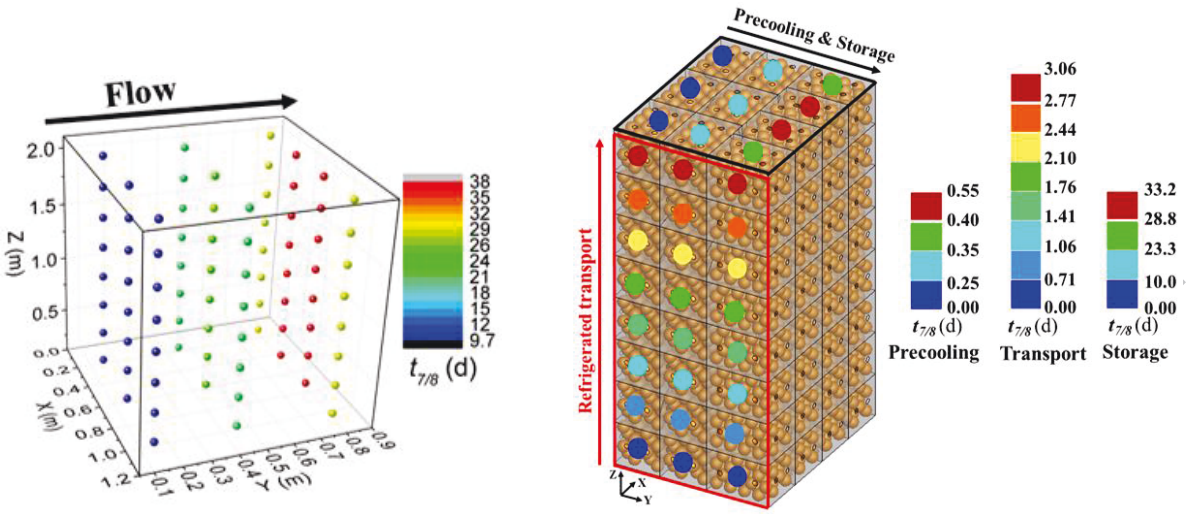

Fig. 8 Spatial distribution of seven-eighth cooling/heating time ($t_{7/8}$) for each box during precooling, transport & storage. $t_{7/8}$ is based on average of core temperature of all fruit in a single carton.

(a) Precooling **(b) transport**

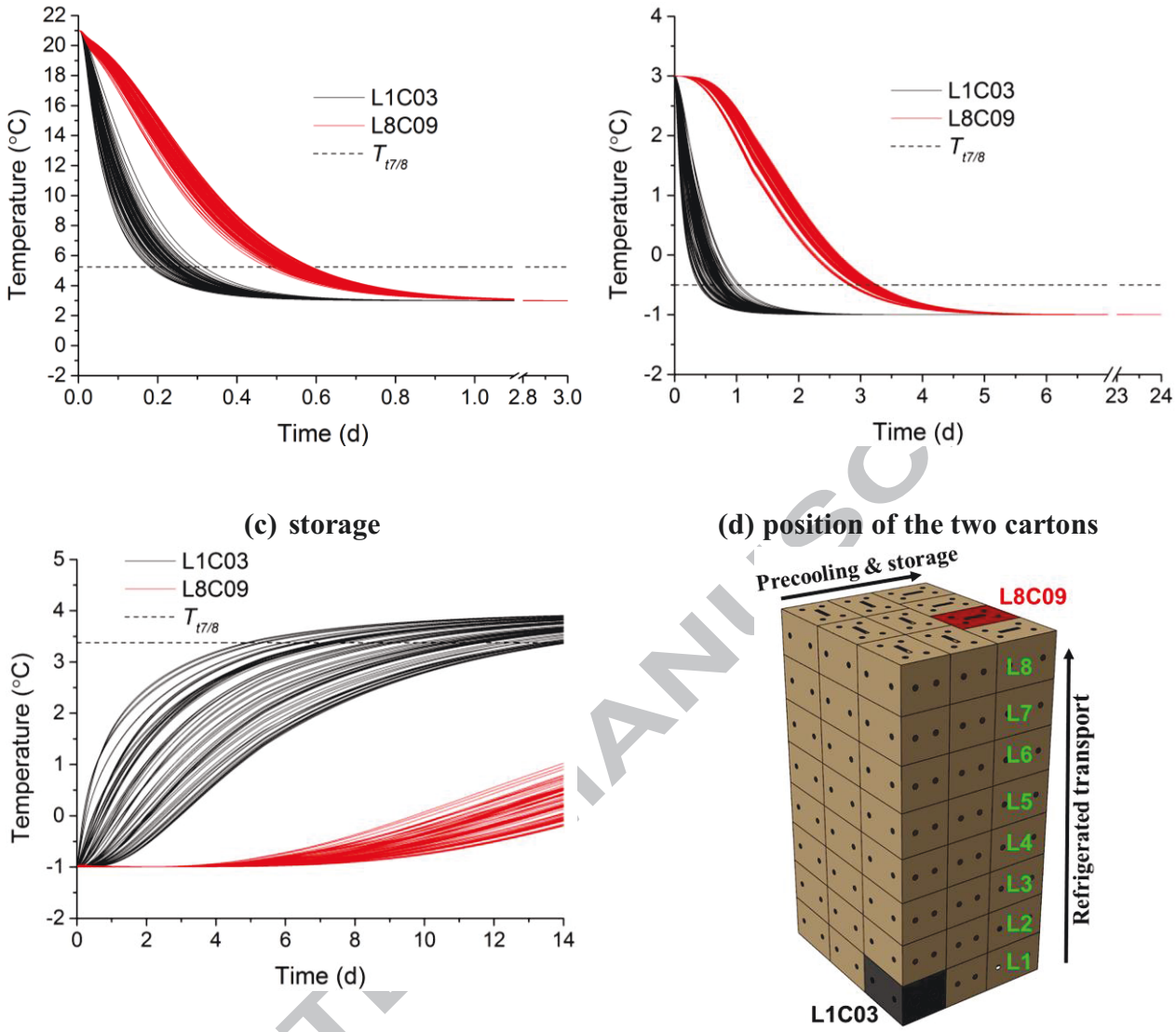

Fig. 9 Core temperature-time history of each individual fruit in carton L1C03 and L8C09 during each unit operation (Precooling, transport and storage). $T_{t7/8}$- temperature at seven eighths cooling/heating time ($t_{7/8}$), that is, one eighths of set point temperature.

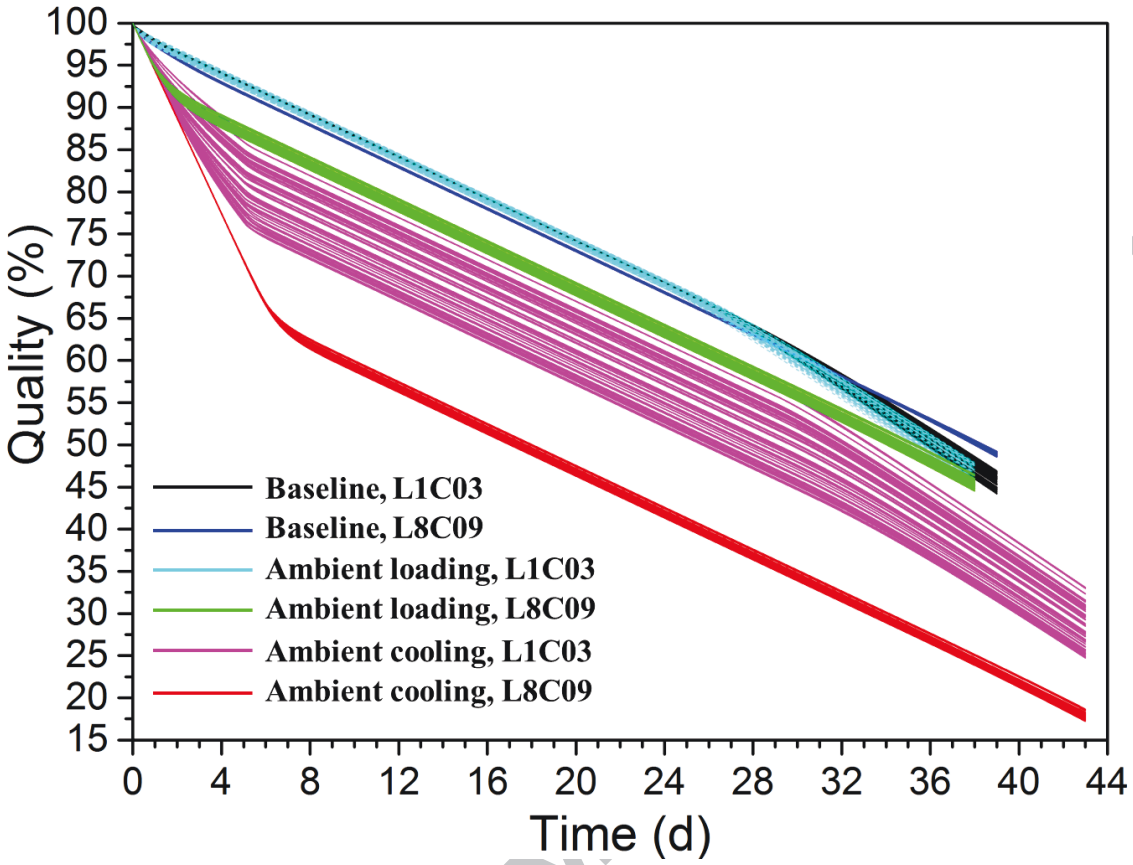

Fig. 10 Quality loss of individual fruit in cartons L1C03 and L8C09 (Fig. 9d) throughout the three cold chains – baseline, ambient cooling and ambient loading.

Table 1 Different cold chains.

Cold chain	Precooling			Cold storage before shipment			Refrigerated transport			Cold storage after shipment		
	Air flow rate (L $kg^{-1}s^{-1}$)	Set point temperature (°C)	Duration (days)	Air flow rate (L $kg^{-1}s^{-1}$)	Set point temperature (°C)	Duration (days)	Air flow rate (L $kg^{-1}s^{-1}$)	Set point temperature (°C)	Duration (days)	Air flow rate (L $kg^{-1}s^{-1}$)	Set point temperature (°C)	Duration (days)
Baseline	0.2	3	1	-	-	-	0.02	-1	24	0.002	4	14
Ambient cooling	-	-	-	0.002	3	5	0.02	-1	24	0.002	4	14
Ambient loading	-	-	-	-	-	-	0.02	-1	24	0.002	4	14

- The cold chain does not contain the corresponding unit operation.

Highlights

- Heterogeneous airflow distribution in the pallet is visualised.
- Cooling heterogeneity along the airflow direction in a pallet is identified.
- Larger cooling heterogeneity among individual fruit occurs in upstream cartons.
- Difference in quality loss is small for fruit in cold chains with precooling.
- Cold chains without precooling have about 23% more quality loss.